

Theory overview of electroweak physics at hadron colliders

John Campbell*

Fermilab, Batavia, IL 60510, USA[†]

E-mail: johnmc@fnal.gov

This contribution summarizes some of the important theoretical progress that has been made in the arena of electroweak physics at hadron colliders. The focus is on developments that have sharpened theoretical predictions for final states produced through electroweak processes. Special attention is paid to new results that have been presented in the last year, since LHCP2015, as well as on key issues for future measurements at the LHC.

*Fourth Annual Large Hadron Collider Physics
13-18 June 2016
Lund, Sweden*

*Speaker.

[†]FERMILAB-CONF-16-336-T

1. Overview

In Run 2 of the LHC a large portion of the experimental program will be devoted to performing a detailed examination of the newly-discovered Higgs boson and to probing the boundaries of the Standard Model (SM). In this vein, precision studies of the mass, couplings and decay modes of the Higgs boson, together with continued searches for supersymmetry, other signs of New Physics and dark matter will be paramount. The vast amount of top quarks collected in the run will also allow its production and decay characteristics to be scrutinized like never before. In order to carry out this rich physics program it will be essential to understand in great detail another class of processes that can be loosely termed *electroweak*: the production of vector bosons (γ , W - or Z -bosons) either singly, in pairs or at even higher multiplicities, possibly in association with additional hadronic activity (jets). Such processes provide important, often irreducible, backgrounds to the aforementioned measurements and searches. These must be understood and checked in great detail in order to best leverage data from the LHC Run 2. Beyond such pragmatic considerations, these processes have their own intrinsic interest that spans from precision measurement of SM parameters to direct tests of the nature of the electroweak sector. Pinning-down the parameters of the SM through measurements of the W -mass and the weak mixing angle has been discussed elsewhere at this conference¹. Related topics, such as making improved determinations of parton distribution functions through precise measurements of electroweak processes, have been touched on by many speakers. A different direction is represented by attempts to explore whether the electroweak sector, as it is currently understood, is a complete description of the theory. This encompasses both searches for anomalous gauge boson couplings and tests of the unitarity-cancellation mechanism in the SM, which can be probed in both inclusive vector boson production and in vector boson scattering [1]. Recent advances in understanding the relevant theoretical challenges in addressing these questions will be detailed in this contribution.

The plethora of measurements of electroweak cross-sections at the LHC, both in Run 1 and in the early results at 13 TeV, have revealed a picture that is very consistent with theoretical predictions of the SM (Figure 1). This impressive agreement, the result of a great deal of concerted effort on both the experimental and theoretical sides, raises an interesting conundrum. The more this agreement persists, the more precision is required on both sides in order to exclude subtle deviations smaller than current uncertainties. It is therefore important to understand the current level of theoretical understanding of these processes, their inherent limitations and the prospects for further improvement. This typically involves not only higher-order calculations in QCD, but also the calculation of electroweak corrections. The combination of these two effects, together with their inclusion in fully-fledged event generators, will be a recurrent theme here. In addition, as the theoretical description becomes more sophisticated, it is important to understand which remaining approximations can be lifted and which of the outstanding uncertainties are most important to control.

2. Drell-Yan processes

Due to their relatively simple nature, these processes have often been at the forefront of theo-

¹See the contribution of M. Schott, “*Precision electroweak physics at hadron colliders*”.

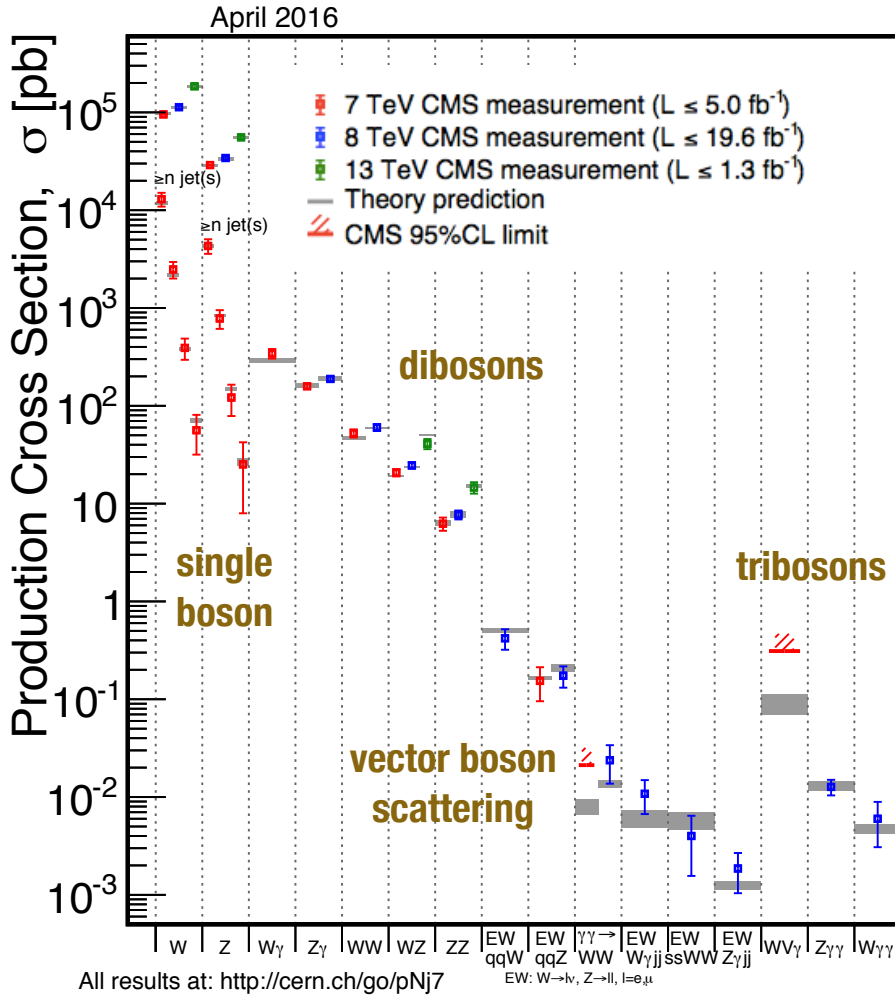


Figure 1: Overview of electroweak cross-sections measured by the CMS experiment, compared with theoretical predictions available in Spring 2016. Minimally-adapted from the CMS TWiki [2].

retical sophistication. Most recently, they have provided the testing-ground for a variety of methods for combining the effects of next-to-next-to-leading (NNLO) QCD corrections with a parton shower. The resulting event generators, SHERPA+BlackHat based on the UN²LOPS method [3], POWHEG using the MiNLO procedure with DYNLO [4] and most recently Geneva(+Pythia) including also NNLL resummation of zero-jettiness [5]², will be indispensable tools in the years to come. Since these techniques are relatively new, it is particularly important that a number of methods have been realized, with slightly different approaches whose merits can be judged directly against LHC data in the future.

At this level of precision it is mandatory to also include the effect of next-to-leading order (NLO) electroweak corrections, that are naively of a similar size (since $\alpha_s^2 \sim \alpha$). Besides this simple argument, there are two distinct kinematic regions that demand a treatment of electroweak

²See the contribution of F. Tackmann, “Drell-Yan production at NNLO+NNLL+PS in Geneva”.

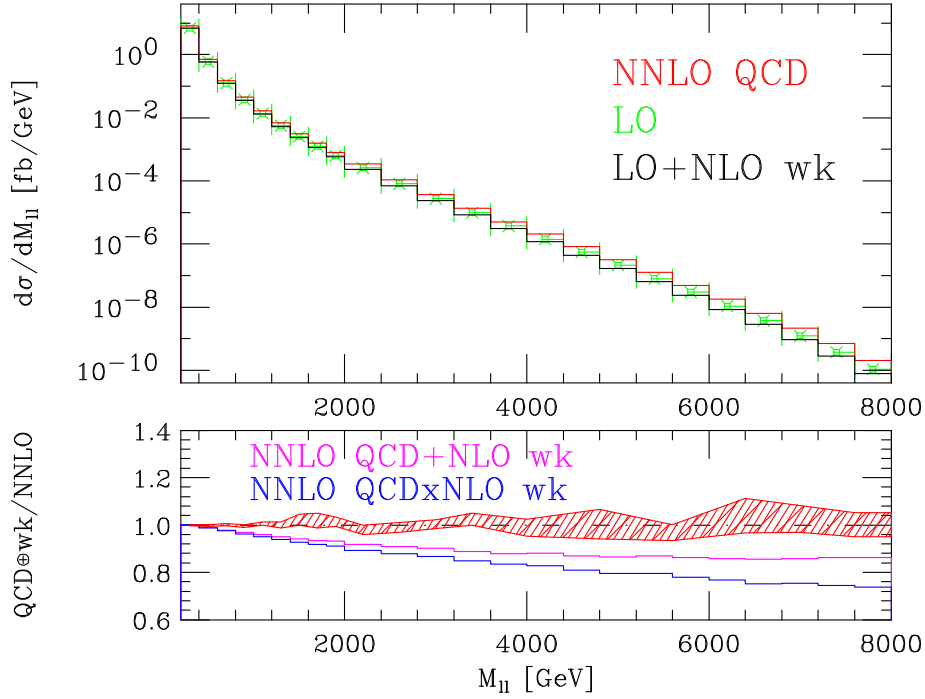


Figure 2: The dilepton invariant mass distribution in 13 TeV collisions predicted at LO (green), NNLO QCD [6] (red, including scale variation) and with NLO weak effects [7] (black). The lower panel shows the difference between the multiplicative (blue) and additive (magenta) combination procedures of NNLO QCD and NLO weak effects (c.f. Eq. (2.2)).

effects. The first is in the region of resonant W or Z production where, in particular, corrections due to the emission of real photons have a significant effect on the line-shape. The second case where electroweak effects become important is in the region of high invariant mass of the vector boson decay products, \hat{s} . The calculation included in the Monte Carlo code FEWZ [8] accounts for corrections through both NNLO QCD and NLO EW and can be used to study the impact of electroweak effects in both regions. In the high-mass region the one-loop electroweak corrections display an enhancement due to Sudakov logarithms whose leading term corresponds to a factor $\log^2(\hat{s}/M_V^2)$, where M_V is the vector boson mass [9]. Defining the individual QCD and weak higher-order corrections relative to the LO result by,

$$r^{QCD}(M) = \frac{d\sigma^{(NNLO\ QCD)}/dM}{d\sigma^{LO}/dM}, \quad r^{wk}(M) = \frac{d\sigma^{(NLO\ wk)}/dM}{d\sigma^{LO}/dM}, \quad (2.1)$$

there are two clear strategies for forming a combined correction. These are,

$$r^{QCD \times wk} = r^{QCD} \times r^{wk} \quad \text{and,} \quad r^{QCD + wk} = r^{QCD} + r^{wk} - 1. \quad (2.2)$$

The size of the individual corrections in the high-mass region means that the choice of either of these procedures for combining NNLO QCD and NLO weak effects gives rise to a significant ambiguity. The difference between the two combinations is outside typical NNLO QCD scale uncertainties and reaches the 10% level for very high dilepton invariant masses (Figure 2). While

such an uncertainty may be adequate given the current data set, it will be untenable in the near future.

A way forward is of course to abandon any approximate combination, instead calculating exactly the class of diagrams that provides a simultaneous enhancement by both couplings. The first such correction, of order $\alpha\alpha_s$, would correspond to a systematic improvement over combining NLO calculations at each order. Such a calculation entails the computation of two-loop diagrams that contain loop propagators corresponding to both strong and weak particles. Although the corresponding master integrals are known [10], a full calculation in this approach is not yet possible. However, results for the mixed QCD-EW corrections have been obtained very recently by using the pole approximation [11]. Compared to a naive combination of QCD and EW corrections, this calculation shows small but significant differences, for instance in the transverse mass distribution of the W -boson. This distribution is pivotal for an extraction of the W -mass and any change in the shape of the theoretical prediction leads to a systematic shift in the extracted value of M_W . The study of Ref. [11] suggests that the mixed QCD-EW corrections could lead to a change in the measured value of M_W by as much as 10 MeV. Since this is comparable to the precision that may be achieved in future at the LHC, it is imperative that this effect be included.

An alternative approach to addressing the issue of QCD and EW corrections simultaneously becoming large can be provided by using a multijet merging procedure in a parton shower [12].³ In this calculation, electroweak and QCD effects are computed for both $V + 1$ and $V + 2$ jet final states, then the results are combined using the usual SHERPA merging of samples. Compared to a strictly fixed-order approach, the ambiguity associated with the combination of QCD and EW corrections is greatly reduced, to a much more palatable level (Figure 3).

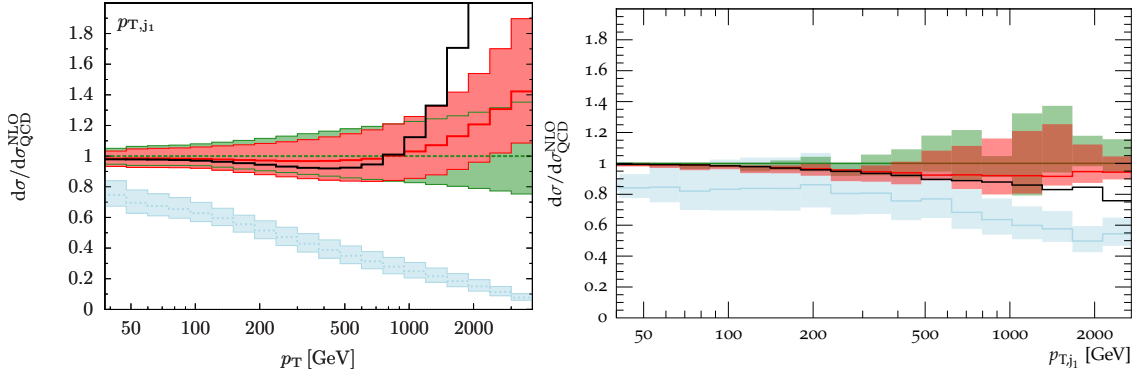


Figure 3: The effect of combining NLO QCD and EW corrections on the lead jet transverse momentum distribution in $W(\rightarrow \ell^- \bar{\nu}) + \text{jet}$ production, in a fixed-order calculation (left) and after merging samples of $V + 1, 2$ jets using the MEPS procedure (right) [12]. The spread in the range of predictions in the right-hand plot is much reduced compared to that on the left.

One of the significant theoretical breakthroughs in perturbative QCD in the last year has been the ability to perform NNLO QCD calculations of $V + \text{jet}$ processes. An important cross-check of the calculations is that they have been performed using both antenna subtraction [13, 14] and

³See the contribution of M. Schoenherr, “NLO QCD+EW for $V + \text{jets}$ ”.

jettiness subtraction [15, 16, 17]. The NNLO calculations enable a much-improved theoretical description of, for instance, the transverse momentum distributions of the Z-boson and the associated jet. The importance of such distributions has been emphasized more than once at this meeting⁴, which is due to the fact that experimental measurements can be made with percent-level precision up to transverse momenta of about 200 GeV. At present some tension with ATLAS Run I data remains [14], even after normalizing by the inclusive Z-boson cross-section in order to remove ambiguities associated with the uncertainty in the total luminosity (Figure 4). The combination of such exquisite data with the sophisticated NNLO predictions, with uncertainties that are only a little larger, offers the opportunity for future parton distribution function constraints in this channel.

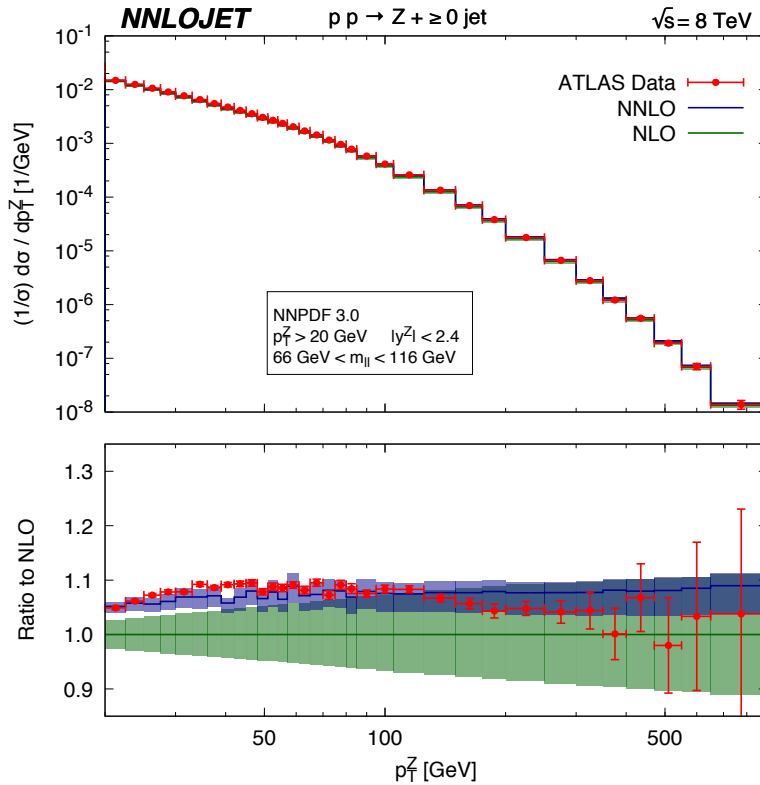


Figure 4: Comparison of the Z-boson transverse momentum through NNLO QCD with data taken at 8 TeV by the ATLAS experiment [14].

3. Diboson production

At the LHCP conference in 2015, theoretical predictions for diboson production were already very advanced, with significant breakthroughs in recent years allowing the computation of many of these processes in NNLO QCD. In the intervening year yet more progress has been made, with

⁴See the contributions of G. Salam, “Theory overview of QCD physics at hadron colliders” and R. Boughezal, “Developments in QCD high order calculations”.

Process	LHCP 2015 status	New developments	Comments
$\gamma\gamma$	NNLO QCD [18]	NNLO(+) QCD [19]	independent calculation; improved treatment of gg contribution
$V\gamma$	NNLO QCD [20] NLO EW ($W\gamma$) [21]	NLO EW ($Z\gamma$) [22]	includes off-shell effects, radiation from leptons in decay
WW	NNLO QCD [23] NLO EW (approx.)	NNLO QCD [24] beyond NNLO QCD [25] NLO EW [26]	single-resonant diagrams, same-flavor lepton ZZ contributions; higher-order gg loops, exact EW
WZ	NLO QCD NLO EW (on-shell)	NNLO QCD [27]	off-shell effects, single-resonant diagrams
ZZ	NNLO QCD [28] NLO EW (approx.)	beyond NNLO QCD [29] NLO EW [30]	higher-order gg loops, exact EW

Table 1: Summary of the status of theoretical calculations of diboson production at the time of LHCP 2015 and the developments since then.

NNLO QCD and NLO EW corrections now computed for all processes. In addition, various refinements – removing previous approximations that had been used – have been implemented, together with first results for a class of important contributions that enters in N^3 LO QCD. The situation is summarized in Table 1.

Many of the new diboson NNLO calculations in the last year have been performed using a general framework called MATRIX [27, 24]⁵. In some cases the new calculations have extended the applicability of previous results, for instance by including off-shell effects in the vector boson decays and accounting for the contribution of single-resonant diagrams. This can have important consequences, for instance on the acceptance (the ratio of the fiducial to inclusive cross-section) predicted by theory. In the case of WW production, the acceptance decreases by approximately 3% when moving from NLO to NNLO, for typical LHC analyses at both 8 and 13 TeV [24]. The missing diboson process, WZ production, was also completed this year [27] and agrees well with LHC data taken at a variety of energies (Figure 5).

Full NLO electroweak corrections have also recently been presented for the cases of $Z\gamma$, WW and ZZ production. In each case important phenomenological consequences of the results of these calculations have been observed. As a first example, consider ATLAS data taken in the $Z\gamma$ channel during Run 1 of the LHC [31] (Figure 6, left), which shows that there is ample data for photon transverse momenta up to about 200 GeV. Comparing with the calculation of NLO EW effects up to this momentum scale (Figure 6, upper right), it is clear that they are rather mild (as large as -10%) in Run 1 [22]. However this will no longer be the case in Run 2, where cross-sections and data samples will be much larger and higher transverse momenta will be probed. An additional observation is that, in some cases – for instance after application of a jet veto, as in the example

⁵See the contribution of S. Kallweit, “NNLO di-boson production”.

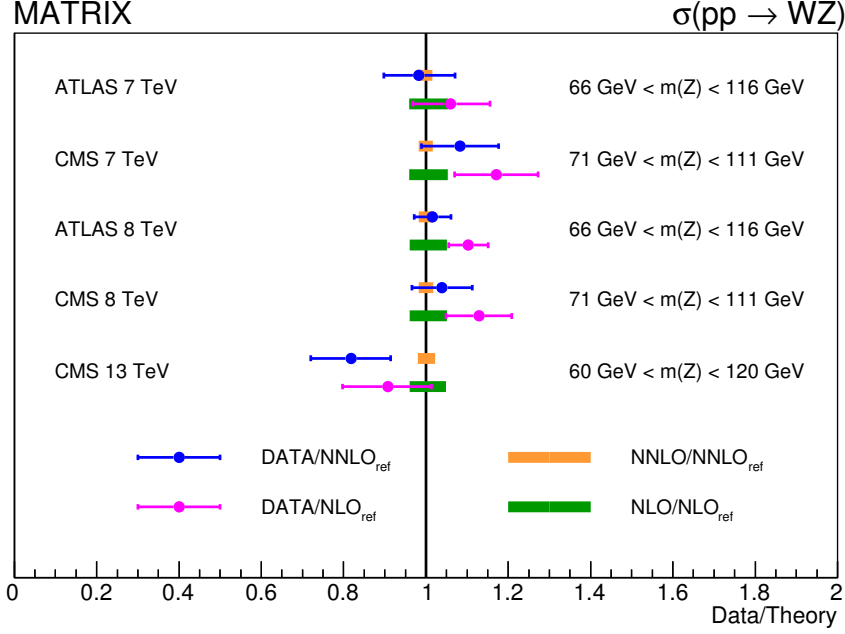


Figure 5: A NNLO calculation of WZ production, compared with experimental measurements performed by ATLAS and CMS at various LHC operating energies [27].

at hand – the NLO EW corrections can become the leading effect, larger than the effect of NLO QCD. A final example underscores once again the importance of a calculation that extends beyond the on-shell case, to full off-shell accuracy (Figure 6, lower right). In this case such a calculation of the ZZ cross-section shows that the behaviour of the EW corrections is very different (opposite in sign) between the on-shell ($M_{4\ell} \sim 2M_Z$) and Higgs search ($M_{4\ell} \sim M_H$) regions [30].

One of the interesting aspects of the theoretical predictions for gauge boson pair production at NNLO is the sensitivity to gg initial states in the neutral channels, i.e. $gg \rightarrow W^+W^-, ZZ$ or $\gamma\gamma$. Such contributions enter through diagrams containing a closed loop of quarks, as shown in Figure 7. Since the SM contains no tree-level coupling of the form ggV_1V_2 it is clear that, despite representing one-loop contributions, these diagrams are finite. The resulting impact on the total cross-section is small, dwarfed by initial states containing quarks, but is important at the level of the corrections that enter at NNLO. In fact these represent the most important NNLO effect in the case of ZZ production [28]. Given this importance at NNLO it is worthwhile to consider whether this contribution, which is included for the first time and therefore suffers all the foibles of a leading order calculation, could be computed at the next order of perturbation theory.

Corrections at the next order (NLO) for the gg -induced components (i.e. entering the full calculation at $N^3\text{LO}$), were first considered for the case of light quark loops in diphoton production [32, 33]. A recent independent calculation of the diphoton process at NNLO has taken into account the leading effect of heavy quark loops and also included the partial $N^3\text{LO}$ effects for loops of light quarks [19]. The partial $N^3\text{LO}$ effects can have as large as a 5-10% effect on the cross section at small diphoton invariant masses and they slightly improve the description of 7 TeV data

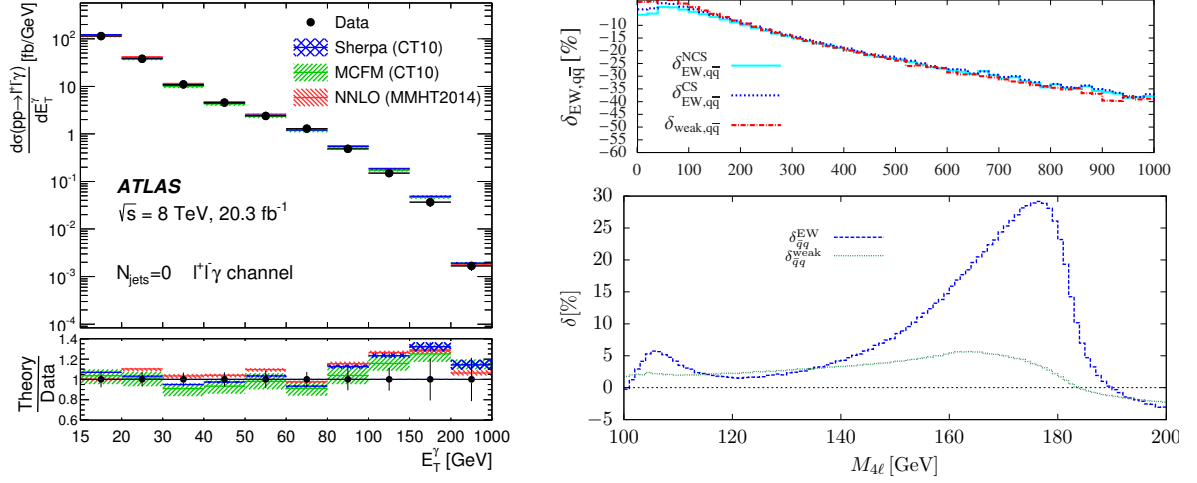


Figure 6: Illustrations of the impact and importance of NLO electroweak corrections to diboson processes: (left) an ATLAS analysis of $l^+l^-\gamma$ events [31]; (upper right) EW effects in the same channel [22]; (lower right) EW effects in ZZ production [30].

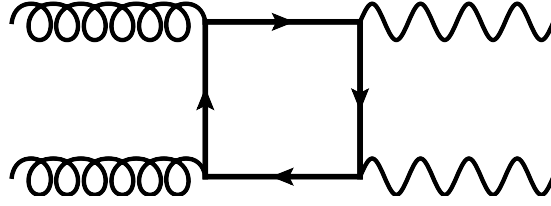


Figure 7: A one-loop diagram representing the process $gg \rightarrow V_1V_2$ that enters the NNLO QCD calculation of V_1V_2 production.

presented by the CMS experiment [34]. The top quark loops have a smaller effect and sculpt the shape of the $m_{\gamma\gamma}$ distribution in the 300 – 500 GeV region. However the effects are far too small to significantly affect the description of the $m_{\gamma\gamma}$ distribution in the region of 750 GeV, where both ATLAS and CMS had indicated a slight excess at the beginning of Run 2 of the LHC [35, 36]. In fact the NNLO calculation provides an excellent *ab initio* calculation of this distribution that agrees very well with the fitting form that had been used by ATLAS and CMS, albeit without any attempt to account for fake rates or efficiencies. A comparison of the ATLAS data and fitting form with the NNLO prediction is shown in Figure 8.

The effect of NLO corrections to the gg contribution to W^+W^- and ZZ final states is considerably harder to compute due to the non-zero W and Z boson masses. Nevertheless, such calculations have been completed in the last year, including the effect of the vector boson decays [29, 25]. In both cases the calculations have, in the first instance, been limited to loops that do not contain the top quark (thus neglecting the entire third generation for W^+W^- production). The effect of the corrections is illustrated in Table 2. The results for ZZ production are shown in the case when no cuts are applied on the Z decay products. In this case the gg contribution increases by almost a factor of two at NLO, but the effect on the overall rate is much smaller, about a 5% enhancement. For

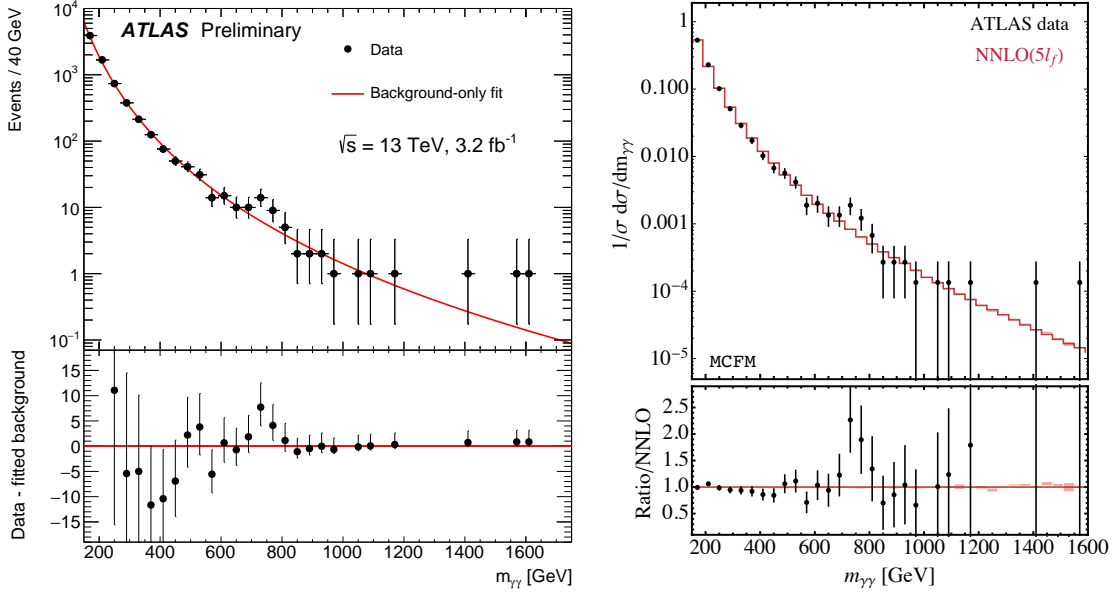


Figure 8: A comparison of diphoton data from the ATLAS experiment and accompanying phenomenological fit [35] (left) with a NNLO calculation [19] (right).

Final-state (cuts)	σ_{gg}^{LO}	σ_{gg}^{NLO}	σ^{NNLO}	$\sigma^{NNLO} + \Delta\sigma_{gg}^{NLO}$
ZZ (no cuts)	0.53 pb	0.95 pb	8.28 pb	8.70 pb
W^+W^- (fiducial cuts) [37]	9.8 fb	11.8 fb	355 fb	357 fb

Table 2: The effect of NLO corrections to gg contributions in vector boson pair production. The final column shows the prediction that includes the full NNLO result and the NLO corrections to the gg channel, with $\Delta\sigma_{gg}^{NLO} = \sigma_{gg}^{NLO} - \sigma_{gg}^{LO}$.

W^+W^- production the cross-sections are shown after the application of fiducial cuts (taken from Ref. [37]), which include a veto on additional jet activity. This greatly reduces the effect of the NLO corrections in this case, resulting in a negligible change in the best theoretical prediction for the cross-section. Note that, even in the case of ZZ production where the impact of the gg loops is biggest, the best measurements from Run 1 suffer from approximately 10% uncertainties [38, 39] and thus are not yet sensitive to such corrections.

4. Off-shell Higgs boson studies

One of the prime modes for making precision measurements of properties of the Higgs boson is the process $gg \rightarrow H \rightarrow ZZ^* \rightarrow 4\ell$. This combination of production and decay modes leads to a substantial cross-section that is under good experimental control. On the theoretical side there has been renewed interest in a precision calculation of this process in the region where the Higgs boson is significantly off-shell. This was first motivated by the fact that a significant fraction, up to 15%, of such events occur in the region $m_{4\ell} > 2m_Z$ [40]. Further interest was provided by the realization

that, in the SM, the ratio of the off-shell and on-shell rates is approximately proportional to the width of the Higgs boson [41]. In order to make use of this observation it is clearly imperative to have precise control of the theoretical prediction. In the off-shell region this means not only the calculation of the diagrams involving the Higgs boson, but also of the $gg \rightarrow ZZ \rightarrow 4\ell$ quark loops such as the one in Figure 7. These diagrams enter at the same order in perturbation theory and make a significant contribution. They interfere destructively and, in the case of the top quark loops, this is essential in order to render the high-energy behavior sensible [42].

Unfortunately, the calculation of the off-shell rate through gg initial states is complicated by the fact that it occurs at leading order through a one-loop process. As discussed already, the leading order nature of this contribution means that it suffers from substantial scale dependence. This means that, for instance, constraints on the Higgs boson width or generic off-shell couplings are weakened by significant theoretical uncertainty [43]. As noted above, the calculation of higher-order corrections, that should include loops of top quarks, is beyond the reach of current technology. In the absence of such predictions, a reasonable assumption is that the higher-order corrections to loop diagrams such as the one in Figure 7 should behave like the corrections to the Higgs diagrams alone (that are, of course, known). This is the basis for a pragmatic estimate of limits on the Higgs boson width as a function of the unknown NLO K -factor [44].

Although an exact calculation of higher-order corrections involving top quark loops is not yet available, the last year has seen significant progress towards this goal. From approximations based on soft gluon resummation [45] to those based on an expansion in inverse powers of the top quark mass [46, 47] (possibly including further refinements [48]), a consensus is emerging. All of these calculations suggest that, in the region of interest, the K -factor for these contribution is indeed very similar to the one for the Higgs diagrams alone. This is shown, for example, in Figure 9, taken from Ref. [47]. Although the K -factors (shown in the lower panels) are significantly different close to the $2M_Z$ threshold – a fact that appears to be due to the contribution of loops of massless quarks – in the highest energy bins they are very similar. This leads to a ratio of off-shell to on-shell production at NLO that is very close to the ratio obtained at LO, except of course with much smaller scale uncertainty [48].

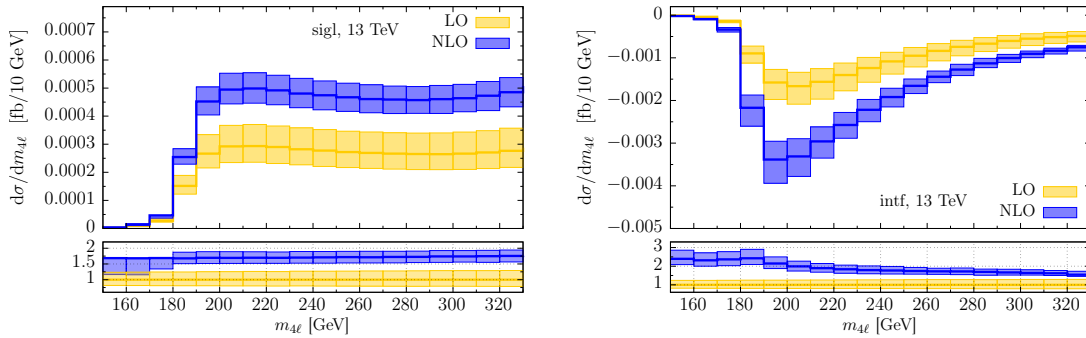


Figure 9: The four-lepton invariant mass distribution for $gg \rightarrow ZZ$ contributions from the Higgs diagrams alone (left) and interference with other one-loop contributions (right). Predictions taken from Ref. [47].

5. Beyond inclusive diboson production

Although the inclusive production of dibosons provides a detailed test of perturbative QCD and has enabled stringent limits on anomalous triple gauge boson couplings to be placed, as the LHC collects more data it will become increasingly sensitive to new mechanisms of vector boson production. These relatively-unexplored channels represent either less inclusive final states or the production of more than two vector bosons.

In the first case, a class of processes that has attracted theoretical interest for a long time [1] is vector boson scattering. At a hadron collider such as the LHC, these processes can be pictured as the emission of a vector boson from each incoming parton, with the bosons subsequently interacting through the weak coupling and two bosons emerging. This picture corresponds to the Feynman diagram shown in Figure 10 (a), with the final state consisting of a pair of bosons and two (mostly forward) jets. However it should be noted that a full gauge-invariant treatment of this process also includes diagrams of the form shown in Figure 10 (b). These enter at the same order ($\mathcal{O}(\alpha^3)$) but contain no gauge boson self-interactions. In addition there are also contributions that involve the Higgs boson (Figure 10, (c) and (d)). In the Higgs boson resonance region the contribution of diagrams of type (c) might normally be accounted for separately, to a very good approximation, as the vector boson fusion process. Finally, there are also QCD-induced contributions ($\mathcal{O}(\alpha_s\alpha^2)$) such as those shown as (e) and (f) of Figure 10. At the very least these diagrams constitute a non-negligible background. In the case of contributions such as (e), which share the same external particles as those of (a)–(d), the QCD and electroweak contributions interfere and a strict separation between the two types of contribution is not meaningful.

It is interesting to note that contribution (d) means that it is possible to retain sensitivity to Higgs boson couplings even without the presence of an s -channel resonance, for instance in the case of like-sign W -boson production. In fact this can be exploited to study off-shell Higgs boson couplings in a similar manner as for inclusive diboson production discussed above. Although the rate is much smaller in vector boson scattering channels, they are tree-level processes and therefore theoretically simpler. These channels also have a greater sensitivity at high energies. The like-sign W channel is particularly promising since the signal suffers from much smaller QCD-induced backgrounds. For instance, Ref. [49] uses ATLAS evidence for $W^\pm W^\pm$ production [50] to obtain a weak bound on the width of the Higgs boson.

In the last few years there has been much work on developing tools that provide concrete predictions for signals of vector boson scattering in extensions of the SM. For instance, the VBFNLO program provides a full suite of predictions for these processes at NLO, including vector boson decays, off-shell effects and anomalous couplings [51].⁶ Other recent work has focussed on extensions that include an additional Higgs singlet or new resonances [52, 53]. An alternative approach is to introduce an effective field theory (EFT) that contains higher-dimension operators that modify the interactions that occur in vector boson scattering processes.⁷ For example, the study in Ref. [54]

⁶The VBFNLO program was also discussed in the contribution of R. Roth, “Anomalous couplings in WZ production beyond NLO QCD”.

⁷For further details see the contribution of M. Sekulla, “Effective Field Theory and Unitarity in Vector Boson Scattering”.

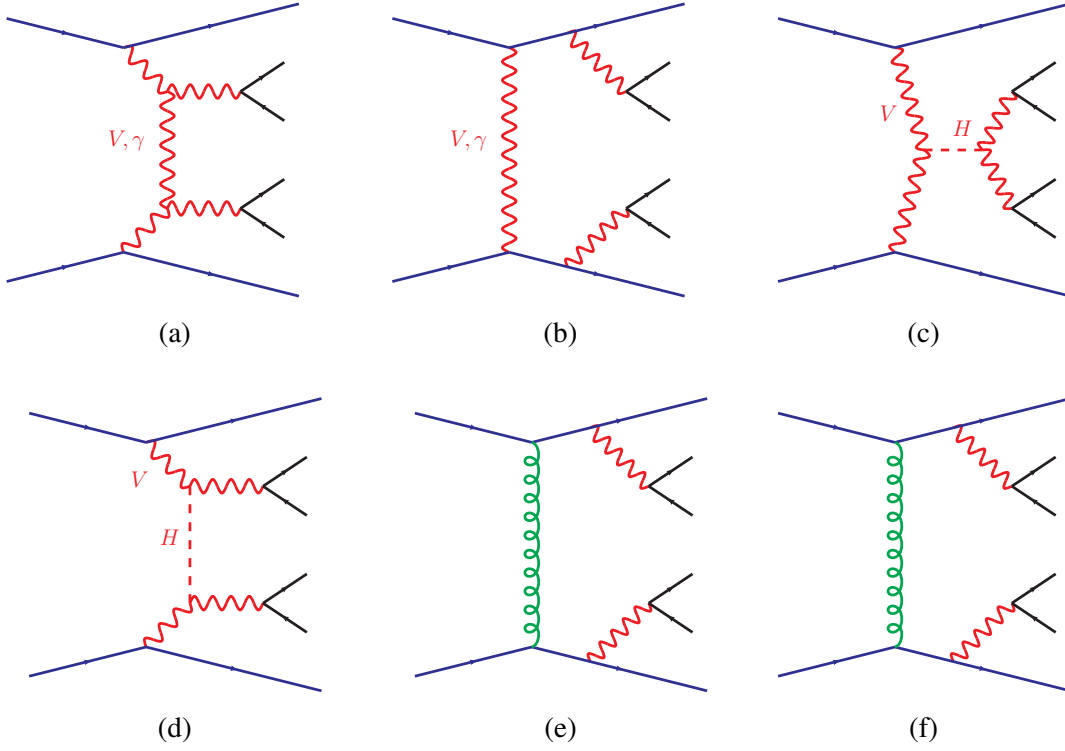


Figure 10: Categories of Feynman diagrams that enter a full calculation of vector boson scattering; (a),(b) vector boson scattering or emission through weak interactions; (c),(d) Higgs boson production or exchange; (e),(f) vector boson production through strong interactions.

has performed a detailed analysis of the effect of additional terms in the Lagrangian of the form,

$$\begin{aligned}
 \mathcal{L}_{HD} &= F_{HD} \operatorname{tr} \left[\mathbf{H}^\dagger \mathbf{H} - \frac{v^2}{4} \right] \cdot \operatorname{tr} \left[(\mathbf{D}_\mu \mathbf{H})^\dagger (\mathbf{D}^\mu \mathbf{H}) \right] \\
 \mathcal{L}_{S,0} &= F_{S,0} \operatorname{tr} \left[(\mathbf{D}_\mu \mathbf{H})^\dagger \mathbf{D}_\nu \mathbf{H} \right] \cdot \operatorname{tr} \left[(\mathbf{D}^\mu \mathbf{H})^\dagger \mathbf{D}^\nu \mathbf{H} \right] \\
 \mathcal{L}_{S,1} &= F_{S,1} \operatorname{tr} \left[(\mathbf{D}_\mu \mathbf{H})^\dagger \mathbf{D}^\mu \mathbf{H} \right] \cdot \operatorname{tr} \left[(\mathbf{D}_\nu \mathbf{H})^\dagger \mathbf{D}^\nu \mathbf{H} \right]
 \end{aligned} \tag{5.1}$$

These interactions lead to bad high-energy behavior, as shown in Figure 11 (left) for the example of W^+W^+jj production at the 14 TeV LHC. The dimension-six operator \mathcal{L}_{HD} , which modifies HW^+W^- and HZZ interactions, only violates unitarity at very high energies, while the other dimension-eight operators (that give rise to modified quartic couplings) do not give reliable predictions at all. One solution is provided by a T -matrix unitarization procedure [54] that tames the growth of the prediction at high energy, as indicated in Figure 11 (right). In the unitarized theory there are still pronounced deviations from the SM expectation, but the rates fall with energy in the same way as in the SM. Understanding the validity of the EFT approach represented by the operators in Eq. (5.1), together with the limitations and uncertainties associated with unitarization procedures such as the one advocated in Ref. [54], will be crucial when interpreting future LHC data on vector boson scattering.

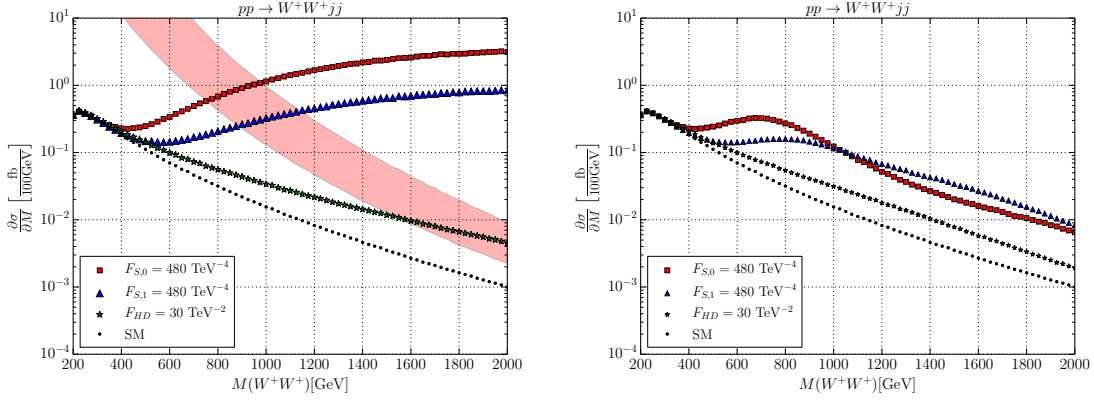


Figure 11: Cross-sections for W^+W^-jj production with the addition of the additional interactions shown in Eq. (5.1). Unitarity is violated for the values of the coupling strengths that cross the pink band (left). After unitarization the high-energy growth is tamed (right).

The production of three or more bosons represents an alternative means of probing anomalous quartic gauge boson couplings. This is an avenue that is only just beginning to be explored at the LHC since the rate for such processes is at the level of a few tens of femtobarns, after branching ratios into experimentally-feasible final states and cuts are applied. For example, the $W\gamma\gamma$ process is one of the most accessible channels and, despite strong evidence, it has so far not been conclusively observed (with more than 5σ significance) by either ATLAS or CMS [55, 56]. From a theoretical point of view this process is interesting because it features the well-known effect of a radiation zero [57]. This effect results in a dip in the distribution of $y(\gamma\gamma) - y(W)$, where $y(\gamma\gamma)$ and $y(W)$ are the rapidities of the $\gamma\gamma$ system and W -boson respectively. At NLO this dip is filled-in, particularly by qg partonic channels that enter for the first time, leading to huge K -factors in this region. This is illustrated in Figure 12 and results in an enhancement of the cross-section for this process by a factor of over three at NLO.

Finally, an important background for studies of top quark production, as well as searches for new physics, is vector boson production in association with jets. The last year has seen calculations of $W^+W^- + \text{jet}$ [58] and $ZZ + \text{jet}$ [59] production that include both QCD and EW effects to NLO. These effects are particularly important to account for at high invariant masses, where searches for new physics or anomalous couplings are typically focussed. In the case of multiple-jet production, the current frontier of perturbative calculations has been pushed as far as $W^+W^- + 3 \text{ jet}$ final states using the combined power of the BlackHat and SHERPA codes [60].

6. Summary

For electroweak processes precision is paramount, both for SM measurements and for probes of subtle effects of new physics. For final states with percent-level experimental precision, such as vector boson and $Z + \text{jet}$ production, theoretical predictions are under control with similar accuracy. This has been achieved through higher-order calculations that are accurate to NNLO in QCD and NLO in electroweak effects, and by the development of new approaches to combining such effects

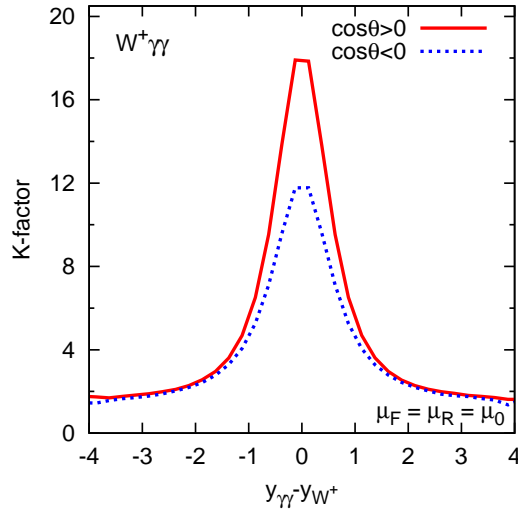


Figure 12: The NLO K -factor for $W^+\gamma\gamma$ production, as a function of the rapidity difference between the $\gamma\gamma$ system and the W^+ -boson, for photons in the same ($\cos\theta > 0$, solid) or opposite ($\cos\theta < 0$, dashed) hemispheres. Figure taken from Ref. [61].

with a parton shower. With more jets in the final state both experiment and theory are a little less pinned-down. Nevertheless, with more data to come and many of the theoretical approaches beginning to be better-understood, prospects for precision probes of the electroweak sector have never been brighter.

Acknowledgments

I thank the organizers for the opportunity to speak at this conference, which was splendidly coordinated and full of excellent and stimulating talks. Fermilab is operated by Fermi Research Alliance, LLC under Contract No. DE-AC02-07CH11359 with the United States Department of Energy.

References

- [1] B. W. Lee, C. Quigg and H. B. Thacker, *Weak Interactions at Very High-Energies: The Role of the Higgs Boson Mass*, *Phys. Rev.* **D16** (1977) 1519.
- [2] “Summary of CMS cross section measurements.”
<https://twiki.cern.ch/twiki/bin/view/CMSPublic/PhysicsResultsCombined>.
- [3] S. Hoeche, Y. Li and S. Prestel, *Drell-Yan lepton pair production at NNLO QCD with parton showers*, *Phys. Rev.* **D91** (2015) 074015, [1405.3607].
- [4] A. Karlberg, E. Re and G. Zanderighi, *NNLOPS accurate Drell-Yan production*, *JHEP* **09** (2014) 134, [1407.2940].
- [5] S. Alioli, C. W. Bauer, C. Berggren, F. J. Tackmann and J. R. Walsh, *Drell-Yan production at NNLL'+NNLO matched to parton showers*, *Phys. Rev.* **D92** (2015) 094020, [1508.01475].

- [6] R. Boughezal, J. M. Campbell, R. K. Ellis, C. Focke, W. Giele, X. Liu et al., *Color singlet production at NNLO in MCFM*, [1605.08011](#).
- [7] J. M. Campbell, D. Wackerth and J. Zhou, *A Study of Weak Corrections to Drell-Yan, Top-quark pair and Di-jet Production at High Energies with MCFM*, [1608.03356](#).
- [8] Y. Li and F. Petriello, *Combining QCD and electroweak corrections to dilepton production in FEWZ*, *Phys. Rev.* **D86** (2012) 094034, [[1208.5967](#)].
- [9] P. Ciafaloni and D. Comelli, *Sudakov enhancement of electroweak corrections*, *Phys. Lett.* **B446** (1999) 278–284, [[hep-ph/9809321](#)].
- [10] R. Bonciani, S. Di Vita, P. Mastrolia and U. Schubert, *Two-Loop Master Integrals for the mixed EW-QCD virtual corrections to Drell-Yan scattering*, [1604.08581](#).
- [11] S. Dittmaier, A. Huss and C. Schwinn, *Dominant mixed QCD-electroweak $O(\alpha\alpha_s)$ corrections to Drell-Yan processes in the resonance region*, *Nucl. Phys.* **B904** (2016) 216–252, [[1511.08016](#)].
- [12] S. Kallweit, J. M. Lindert, P. Maierhofer, S. Pozzorini and M. Schoenherr, *NLO QCD+EW predictions for $V + jets$ including off-shell vector-boson decays and multijet merging*, *JHEP* **04** (2016) 021, [[1511.08692](#)].
- [13] A. Gehrmann-De Ridder, T. Gehrmann, E. W. N. Glover, A. Huss and T. A. Morgan, *Precise QCD predictions for the production of a Z boson in association with a hadronic jet*, *Phys. Rev. Lett.* **117** (2016) 022001, [[1507.02850](#)].
- [14] A. Gehrmann-De Ridder, T. Gehrmann, E. W. N. Glover, A. Huss and T. A. Morgan, *The NNLO QCD corrections to Z boson production at large transverse momentum*, [1605.04295](#).
- [15] R. Boughezal, C. Focke, X. Liu and F. Petriello, *W-boson production in association with a jet at next-to-next-to-leading order in perturbative QCD*, *Phys. Rev. Lett.* **115** (2015) 062002, [[1504.02131](#)].
- [16] R. Boughezal, J. M. Campbell, R. K. Ellis, C. Focke, W. T. Giele, X. Liu et al., *Z-boson production in association with a jet at next-to-next-to-leading order in perturbative QCD*, *Phys. Rev. Lett.* **116** (2016) 152001, [[1512.01291](#)].
- [17] R. Boughezal, X. Liu and F. Petriello, *A comparison of NNLO QCD predictions with 7 TeV ATLAS and CMS data for $V + jet$ processes*, *Phys. Lett.* **B760** (2016) 6–13, [[1602.05612](#)].
- [18] S. Catani, L. Cieri, D. de Florian, G. Ferrera and M. Grazzini, *Diphoton production at hadron colliders: a fully-differential QCD calculation at NNLO*, *Phys. Rev. Lett.* **108** (2012) 072001, [[1110.2375](#)].
- [19] J. M. Campbell, R. K. Ellis, Y. Li and C. Williams, *Predictions for diphoton production at the LHC through NNLO in QCD*, [1603.02663](#).
- [20] M. Grazzini, S. Kallweit and D. Rathlev, *$W\gamma$ and $Z\gamma$ production at the LHC in NNLO QCD*, *JHEP* **07** (2015) 085, [[1504.01330](#)].
- [21] A. Denner, S. Dittmaier, M. Hecht and C. Pasold, *NLO QCD and electroweak corrections to $W + \gamma$ production with leptonic W-boson decays*, *JHEP* **04** (2015) 018, [[1412.7421](#)].
- [22] A. Denner, S. Dittmaier, M. Hecht and C. Pasold, *NLO QCD and electroweak corrections to $Z + \gamma$ production with leptonic Z-boson decays*, *JHEP* **02** (2016) 057, [[1510.08742](#)].
- [23] T. Gehrmann, M. Grazzini, S. Kallweit, P. Maierhofer, A. von Manteuffel, S. Pozzorini et al., *W^+W^- Production at Hadron Colliders in Next to Next to Leading Order QCD*, *Phys. Rev. Lett.* **113** (2014) 212001, [[1408.5243](#)].

- [24] M. Grazzini, S. Kallweit, S. Pozzorini, D. Rathlev and M. Wiesemann, W^+W^- production at the LHC: fiducial cross sections and distributions in NNLO QCD, 1605.02716.
- [25] F. Caola, K. Melnikov, R. Roentsch and L. Tancredi, QCD corrections to W^+W^- production through gluon fusion, *Phys. Lett.* **B754** (2016) 275–280, [1511.08617].
- [26] B. Biedermann, M. Billoni, A. Denner, S. Dittmaier, L. Hofer, B. Jaeger et al., Next-to-leading-order electroweak corrections to $pp \rightarrow W^+W^- \rightarrow 4$ leptons at the LHC, *JHEP* **06** (2016) 065, [1605.03419].
- [27] M. Grazzini, S. Kallweit, D. Rathlev and M. Wiesemann, $W^\pm Z$ production at hadron colliders in NNLO QCD, 1604.08576.
- [28] M. Grazzini, S. Kallweit and D. Rathlev, ZZ production at the LHC: fiducial cross sections and distributions in NNLO QCD, *Phys. Lett.* **B750** (2015) 407–410, [1507.06257].
- [29] F. Caola, K. Melnikov, R. Roentsch and L. Tancredi, QCD corrections to ZZ production in gluon fusion at the LHC, *Phys. Rev.* **D92** (2015) 094028, [1509.06734].
- [30] B. Biedermann, A. Denner, S. Dittmaier, L. Hofer and B. Jaeger, Electroweak corrections to $pp \rightarrow \mu^+\mu^-e^+e^- + X$ at the LHC: a Higgs background study, *Phys. Rev. Lett.* **116** (2016) 161803, [1601.07787].
- [31] ATLAS collaboration, G. Aad et al., Measurements of $Z\gamma$ and $Z\gamma\gamma$ production in pp collisions at $\sqrt{s} = 8$ TeV with the ATLAS detector, *Phys. Rev.* **D93** (2016) 112002, [1604.05232].
- [32] Z. Bern, A. De Freitas and L. J. Dixon, Two loop amplitudes for gluon fusion into two photons, *JHEP* **09** (2001) 037, [hep-ph/0109078].
- [33] Z. Bern, L. J. Dixon and C. Schmidt, Isolating a light Higgs boson from the diphoton background at the CERN LHC, *Phys. Rev.* **D66** (2002) 074018, [hep-ph/0206194].
- [34] CMS collaboration, S. Chatrchyan et al., Measurement of differential cross sections for the production of a pair of isolated photons in pp collisions at $\sqrt{s} = 7$ TeV, *Eur. Phys. J.* **C74** (2014) 3129, [1405.7225].
- [35] ATLAS collaboration, Search for resonances decaying to photon pairs in 3.2 fb^{-1} of pp collisions at $\sqrt{s} = 13$ TeV with the ATLAS detector, Tech. Rep. ATLAS-CONF-2015-081, CERN, Geneva, Dec, 2015.
- [36] CMS collaboration, Search for new physics in high mass diphoton events in proton-proton collisions at $\sqrt{s} = 13$ TeV, Tech. Rep. CMS-PAS-EXO-15-004, CERN, Geneva, 2015.
- [37] ATLAS collaboration, G. Aad et al., Measurement of total and differential W^+W^- production cross sections in proton-proton collisions at $\sqrt{s} = 8$ TeV with the ATLAS detector and limits on anomalous triple-gauge-boson couplings, 1603.01702.
- [38] ATLAS collaboration, Measurement of the total ZZ production cross section in proton-proton collisions at $\sqrt{s} = 8$ TeV in 20 fb^{-1} with the ATLAS detector, .
- [39] CMS collaboration, V. Khachatryan et al., Measurement of the $pp \rightarrow ZZ$ production cross section and constraints on anomalous triple gauge couplings in four-lepton final states at $\sqrt{s} = 8$ TeV, *Phys. Lett.* **B740** (2015) 250–272, [1406.01113].
- [40] N. Kauer and G. Passarino, Inadequacy of zero-width approximation for a light Higgs boson signal, *JHEP* **08** (2012) 116, [1206.4803].

- [41] F. Caola and K. Melnikov, *Constraining the Higgs boson width with ZZ production at the LHC*, *Phys. Rev. D* **88** (2013) 054024, [1307.4935].
- [42] E. N. Glover and J. van der Bij, *Z-boson pair production via gluon fusion*, *Nucl.Phys.* **B321** (1989) 561.
- [43] J. M. Campbell, R. K. Ellis and C. Williams, *Bounding the Higgs width at the LHC using full analytic results for $gg \rightarrow e^-e^+\mu^-\mu^+$* , *JHEP* **04** (2014) 060, [1311.3589].
- [44] ATLAS collaboration, G. Aad et al., *Constraints on the off-shell Higgs boson signal strength in the high-mass ZZ and WW final states with the ATLAS detector*, *Eur. Phys. J.* **C75** (2015) 335, [1503.01060].
- [45] C. S. Li, H. T. Li, D. Y. Shao and J. Wang, *Soft gluon resummation in the signal-background interference process of $gg(\rightarrow h) \rightarrow ZZ$* , *JHEP* **08** (2015) 065, [1504.02388].
- [46] K. Melnikov and M. Dowling, *Production of two Z-bosons in gluon fusion in the heavy top quark approximation*, *Phys. Lett.* **B744** (2015) 43–47, [1503.01274].
- [47] F. Caola, M. Dowling, K. Melnikov, R. Röntsch and L. Tancredi, *QCD corrections to vector boson pair production in gluon fusion including interference effects with off-shell Higgs at the LHC*, *JHEP* **07** (2016) 087, [1605.04610].
- [48] J. M. Campbell, R. K. Ellis, M. Czakon and S. Kirchner, *Two loop correction to interference in $gg \rightarrow ZZ$* , *JHEP* **08** (2016) 011, [1605.01380].
- [49] J. M. Campbell and R. K. Ellis, *Higgs Constraints from Vector Boson Fusion and Scattering*, *JHEP* **04** (2015) 030, [1502.02990].
- [50] ATLAS collaboration, G. Aad et al., *Evidence for Electroweak Production of $W^\pm W^\pm jj$ in pp Collisions at $\sqrt{s} = 8$ TeV with the ATLAS Detector*, *Phys. Rev. Lett.* **113** (2014) 141803, [1405.6241].
- [51] F. Campanario, M. Kerner, L. D. Ninh, M. Rauch, R. Roth and D. Zeppenfeld, *NLO corrections to processes with electroweak bosons at hadron colliders*, *Nucl. Part. Phys. Proc.* **261-262** (2015) 268–307.
- [52] A. Ballestrero and E. Maina, *Interference Effects in Higgs production through Vector Boson Fusion in the Standard Model and its Singlet Extension*, *JHEP* **01** (2016) 045, [1506.02257].
- [53] W. Kilian, T. Ohl, J. Reuter and M. Sekulla, *Resonances at the LHC beyond the Higgs boson: The scalar/tensor case*, *Phys. Rev. D* **93** (2016) 036004, [1511.00022].
- [54] W. Kilian, T. Ohl, J. Reuter and M. Sekulla, *High-Energy Vector Boson Scattering after the Higgs Discovery*, *Phys. Rev. D* **91** (2015) 096007, [1408.6207].
- [55] ATLAS collaboration, G. Aad et al., *Evidence of $W\gamma\gamma$ Production in pp Collisions at $\sqrt{s} = 8$ TeV and Limits on Anomalous Quartic Gauge Couplings with the ATLAS Detector*, *Phys. Rev. Lett.* **115** (2015) 031802, [1503.03243].
- [56] CMS collaboration, *Measurements of The $pp \rightarrow W^\pm\gamma\gamma$ and $pp \rightarrow Z\gamma\gamma$ Cross Sections and Limits on Dimension-8 Effective Anomalous Gauge Couplings at $\sqrt{s} = 8$ TeV*, Tech. Rep. CMS-PAS-SMP-15-008, CERN, 2016.
- [57] K. Mikaelian, M. Samuel and D. Sahdev, *The magnetic moment of weak bosons produced in pp and $p\bar{p}$ collisions*, *Phys.Rev.Lett.* **43** (1979) 746.

- [58] W.-H. Li, R.-Y. Zhang, W.-G. Ma, L. Guo, X.-Z. Li and Y. Zhang, *NLO QCD and electroweak corrections to WW +jet production with leptonic W -boson decays at LHC*, *Phys. Rev.* **D92** (2015) 033005, [[1507.07332](#)].
- [59] Y. Wang, R.-Y. Zhang, W.-G. Ma, X.-Z. Li and L. Guo, *QCD and electroweak corrections to ZZ +jet production with Z -boson leptonic decays at the LHC*, *Phys. Rev.* **D94** (2016) 013011, [[1604.04080](#)].
- [60] F. Febres Cordero, P. Hofmann and H. Ita, *$W^+W^- + 3$ Jet Production at the Large Hadron Collider in NLO QCD*, [1512.07591](#).
- [61] G. Bozzi, F. Campanario, M. Rauch and D. Zeppenfeld, *$W^{+-}\gamma\gamma$ production with leptonic decays at NLO QCD*, *Phys. Rev.* **D83** (2011) 114035, [[1103.4613](#)].